



STATE RESEARCH CENTER OF RUSSIA
INSTITUTE FOR HIGH ENERGY PHYSICS

IHEP 2005-35

S.P. Denisov¹, A. Dzierba², A.K. Klimenko¹, R. Mitchell²,
V.D. Samoylenko¹, E. Scott², P. Smith², S. Teige²

**STUDIES OF TIMING AND AMPLITUDE PROPERTIES
FOR 2 m LONG SCINTILLATION COUNTER
WITH FEU-115M PMT'S ³**

Submitted to *PTE*

¹ Institute for High Energy Physics, Protvino, Russia

² Department of Physics, Indiana University, Bloomington, IN 47405 USA

³ This paper reports on research carried out on behalf of the GlueX/Hall D collaboration at Jefferson Lab in Newport News, VA, USA

Abstract

Denisov S.P., Dzierba A., Klimenko A.K. et al. Studies of Timing and Amplitude Properties for 2 m Long Scintillation Counter with FEU-115M PMT's : IHEP Preprint 2005-35. – Protvino, 2005. – p. 12, figs. 14, refs.: 16.

Timing and signal pulse height characteristics of a scintillation counter were studied using a 5 GeV/c particle beam at the IHEP accelerator. The scintillation bar was 2 m long and had a cross-section of $2.5 \times 2.5 \text{ cm}^2$. It was viewed from both sides by FEU-115M PMT's. The dependences of the signal pulse height and the time resolution on the coordinate along the scintillator are well described by an exponential function with a quadratic term. The counter time resolution was equal to 150 ps and 80 ps at the center and at the edge of the scintillator bar respectively if a constant fraction discriminator was used to avoid the walk-effect. Somewhat better results were obtained for the leading edge discriminator if the signal time and pulse height were measured simultaneously and the walk-effect was corrected off-line.

Аннотация

Денисов С.П., Дзерба А., Клименко А.К. и др. Исследование временных и амплитудных характеристик сцинтилляционного счетчика длиной 2 м с ФЭУ-115М: Препринт ИФВЭ 2005-35. – Протвино, 2005. – 12 с., 14 рис., библиогр.: 16.

В пучке частиц с импульсом 5 ГэВ/с ускорителя ИФВЭ исследованы временные и амплитудные характеристики сцинтилляционного счетчика. Сцинтиллятор имел длину 2 м и сечение $2,5 \times 2,5 \text{ см}^2$. Он просматривался с торцов ф.э.у ФЭУ-115М. Зависимости амплитуды сигнала и временного разрешения ф.э.у. от координаты трека частицы вдоль сцинтиллятора хорошо описываются квадратичной экспонентой. При использовании в качестве формирователя сигнала ф.э.у. дискриминатора постоянной части сигнала временное разрешение в центре и на краях счетчика равно 150 и 80 пс соответственно. Несколько лучшие результаты получены для обычного порогового формирователя после коррекции зависимости времени его срабатывания от амплитуды сигнала.

Introduction

Scintillation counters with good time resolution are widely used in experiments at accelerators and colliders for particle identification by the time-of-flight (TOF) technique and for precise event timing required in high intensity beams [1, 2, 3, 4]. We investigated a prototype scintillation counter to be used in the TOF system of the GlueX experiment [5] at Jefferson Laboratory (Newport News, USA) and in hodoscopes for studies of rare K^+ - decays with hadron beams of 10^8 particles/s at the Institute for High Energy Physics (Protvino, Russia). The scintillator length is 2 m and its cross-section is 2.5×2.5 cm². EL-200 scintillator [6] was used with a decay time of 2.1 ns, a bulk absorption length of 4 m, and an index of refraction of 1.58. The scintillator was viewed from both ends by FEU-115M PMT's with a multialkali photocathode, 20 mm in diameter, produced by the MELZ plant [7] in Moscow. The FEU-115M is used in many experiments in Russia and abroad. More than 20,000 FEU-115M are used in the PHENIX [8] and D0 [9] experiments. Their timing properties are somewhat worse than those of the best Photonics and Hamamatsu PMT's but their cost is considerably lower. In this paper we present the summary of detailed studies of timing properties for the scintillation counter with FEU-115M PMT's. The results of some of those studies were published earlier [10].

1. Apparatus and Measurements

Measurements were performed with the 5 GeV/c hadron beam of the IHEP accelerator. The particle flux was monitored by three beam scintillation counters S1-S3 (Fig. 1). These counters were made of BC-404 [11] scintillator and equipped with XP2020 PMT's [12]. Scintillator S1 was 100 mm in diameter and 12.5 mm thick and the dimensions of the S2 and S3 scintillators were $20 \times 20 \times 12.5$ mm³. Signals from S1-S3 were fed to CF8000 constant fraction discriminators (CFD) [13]. A CFD allows one to avoid the dependence of a discriminator delay on the input signal pulse height, the well known "walk-effect". The best timing was achieved with these CFD parameters: a 4 ns delay, a 30 mV threshold, and a fraction of 0.4.

Signals from the CFD's went to the 3-fold coincidence unit TRG (Fig. 1) and to the 12 bit TDC with a 26.5 ps least count. The coincidence signal was used as a trigger, as a strobe for

the ADC, and as a START signal for the TDC. It was also fed to one of the TDC channels as a STOP signal to determine the intrinsic time resolution of electronics which was measured to be 18 ps. The timing of the START signal was defined by the S2 counter.

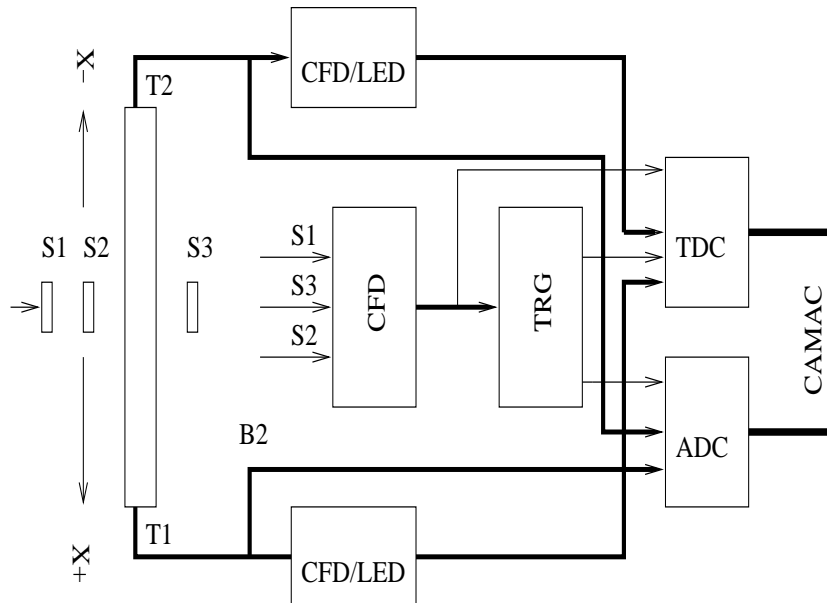


Figure 1. Layout of the counters and the electronics: S1, S2, S3 – beam counters; T1, T2 – PMT's of the test counter; CFD – constant fraction discriminator; LED – leading edge discriminator; TRG – coincidence unit; TDC – time-to-digital converter; ADC – amplitude-to-digital converter.

Fig. 2 shows the time spectrum for this counter. Since S2 and S3 counters are identical one can estimate from a Gaussian fit to the spectrum of Fig. 2 that the trigger time resolution is $\sigma_{tr} = 80 \pm 2$ ps.

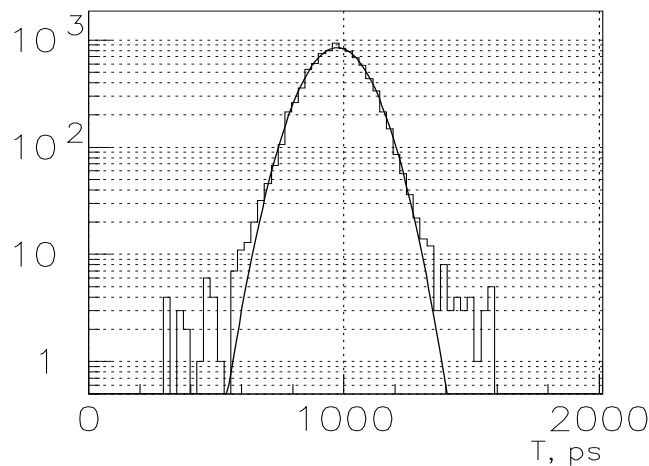


Figure 2. Time distribution of the trigger signals. A Gaussian fit to this distribution yields a time resolution of $\sigma_{tr} = 80 \pm 2$ ps.

The test counter was placed in a light-tight box between S2 and S3. It could be moved in the horizontal (x) direction in 100 mm steps. Bicon grease [11] was used for the optical contact between PMT's and the scintillator bar. The bar was not wrapped as it was shown previously [10] that wrapping with Tyvek or aluminium foil does not influence the time resolution.

T1 and T2 signals were sent via 40 m, 50 Ω cables to 12 bit ADC's with 0.25pC/count sensitivity and constant fraction (CFD) or leading edge discriminators (LED). Signals from the discriminators were used as STOP signals for TDC's.

2. Pulse height measurements

Pulse height and time distributions were measured for PMT signals at different positions of the scintillation bar with respect to the beam axis from $x=0$ (bar center) to ± 90 cm (see Fig. 1). 10,000 events were collected at each x position.

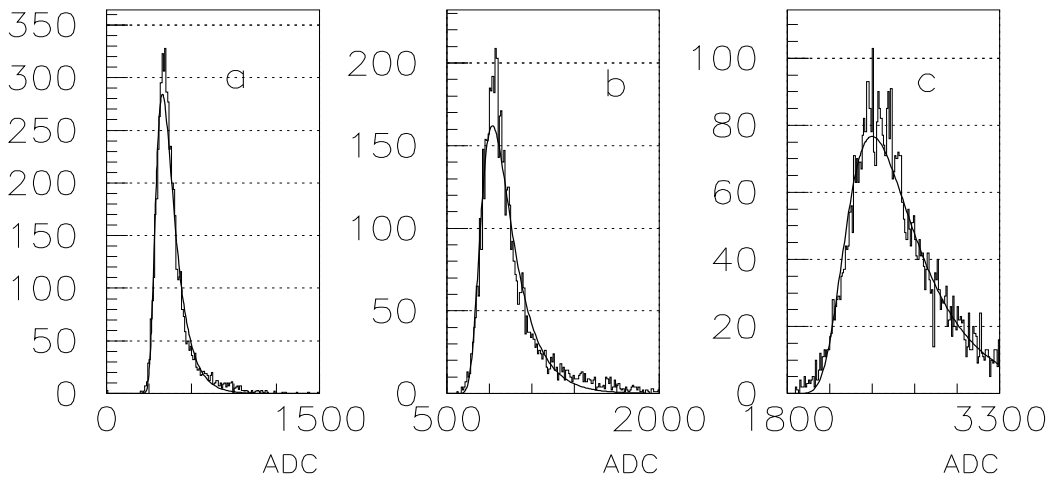


Figure 3. Pulse height spectra of T1 for (a): $x = -60$; (b): $x = 0$ and (c): $x = +60$ cm. Pulse height is measured in ADC's counts. The curves are the results of fits to a Moyal distribution as described in the text.

Fig. 3 shows the T1 pulse height spectra fitted by Moyal distribution which allows one to reconstruct the leading edge and the peak position, denoted by the parameter A . The x -dependence of A is shown in Fig. 4 where the dotted and solid lines represent the relations:

$$A(x) = A_o \exp(x/\lambda_a), \quad (1)$$

$$A(x) = A'_o \exp(x/\lambda'_a + \alpha_a x^2/\lambda_a'^2) \quad (2)$$

with the following parameters calculated by the least square method: $\lambda_a = 68 \pm 1$ cm, $\lambda'_a = 65 \pm 1$ cm, $\alpha_a = 0,17 \pm 0,01$.

From Fig. 4 it is clear that equation (2) fits the experimental data much better than equation (1). The difference between the simple exponential description of equation (1) and the data can be explained by the light reflection from the far end of the bar (small x) and by the increasing of the amount of light reaching the PMT without reflection (large x).

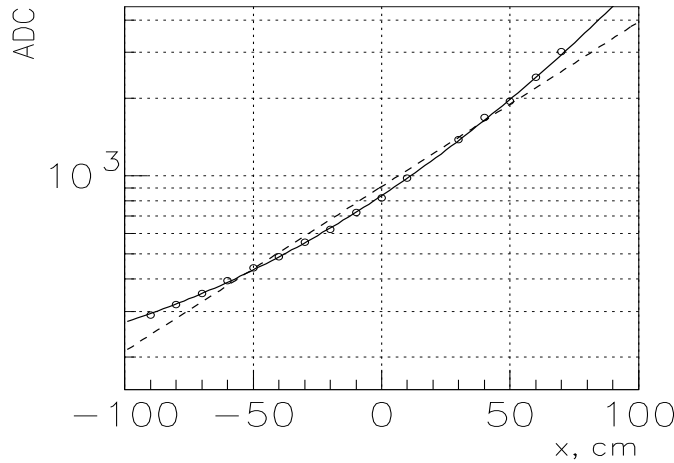


Figure 4. The x -dependence of the average pulse height A for T1. Dotted and solid lines fits to equations (1) and (2). A is measured in ADC counts.

Similar results were obtained for T2. The values of the absorption lengths are much smaller than those expected for the scintillator with bulk attenuation length of $\lambda_b = 4.0$ m and average angle of light with respect to the x axis of $\bar{\theta} = 33.7^\circ$ (see below). The reason for this is that the scintillator polishing is not perfect and light hitting the scintillator surface at an angle greater than the total reflection angle is partially lost.

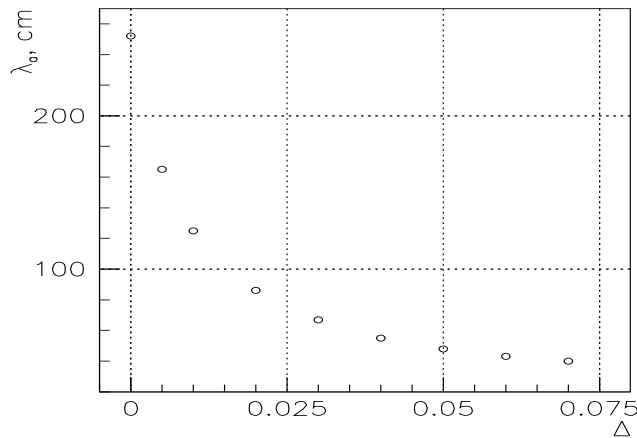


Figure 5. Dependence of the absorption length λ_a on the average light loss per reflection Δ .

Fig. 5 shows λ_a vs light loss per reflection (Δ) obtained by simulation of scintillation light propagation along the bar. From this figure it follows that $\lambda_a = 68$ cm corresponds to $\Delta = 0.03$. In the case of $\Delta \ll 1$, a simple formula can be derived for the absorption length for light moving in the plane parallel to the sides of the scintillator bar of width d and at an angle θ with respect

to the x direction:

$$\frac{1}{\lambda_a} = \frac{1}{\lambda_b \cos \theta} \left(1 - \frac{\lambda_b}{d} \Delta \sin \theta\right). \quad (3)$$

Choosing $\theta = \bar{\theta} = 33.7^\circ$ one can find $\Delta = 0.04$ for $\lambda_b = 400$ cm and $\lambda_a = 68$ cm. This value is in a reasonable agreement with those calculated by Monte Carlo.

To find the relation between the ADC counts and the number N_{ph} of photoelectrons we used the A_1/A_2 and $(A_1 - A_2)/(A_1 + A_2)$ distributions (Fig. 6), where A_1 and A_2 are pulse heights of the signals from T1 and T2. The widths of these distributions depend mainly on photoelectron statistics and weakly on fluctuations of scintillation light intensity. They are not spoiled by the Landau fluctuations of the ionization loss which contribute equally to A_1 and A_2 . Assuming that the quantum yields and gains of T1 and T2 are equal one can estimate that the average number of photoelectrons per PMT at $x = 0$ is $N_{ph} \approx 280$ or one ADC count corresponds to 0.3 photoelectrons.

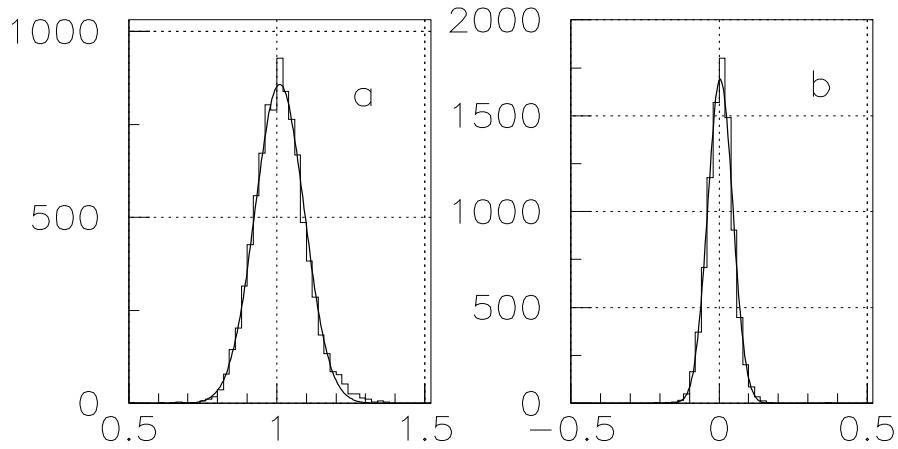


Figure 6. A_1/A_2 (a) and $(A_1 - A_2)/(A_1 + A_2)$ (b) distributions for T1 and T2.

3. Measurements with CFD's

Time distributions of the PMT signals are well fitted by a Gaussian form (see Fig. 7).

The variance and the mean of the Gaussian were used to estimate the time resolution σ_m and the average time T measured by TDC. The dependencies $T(x)$ are shown in Fig. 8. These data allow one to calculate the light velocity V_x along the bar and average angle $\bar{\theta}$ of photons with respect to the x -axis.

For an index of refraction $n = 1.58$ the values obtained are equal to 15.8 cm/ns and 33.7° respectively.

The dependence of σ_m on the distance s between the particle track and the PMT can be presented by the following formula:

$$\sigma_m(s) = \sqrt{(\sigma^2(0) + (\sigma_s s)^2) \exp(2s/\lambda_t) + \sigma_{trm}^2}, \quad (4)$$

where $s = 100 \pm x$ cm ('-' and '+' refer to T1 and T2, respectively), $\sigma(0)$ is the intrinsic time resolution of the PMT at $s = 0$, σ_{trm} is the trigger time resolution, λ_t is a parameter characterizing

the length scale of resolution degradation and the parameter σ_s characterizes the spread of a light bunch during propagation along the bar due to nonisochronous photon trajectories. Fitting to the experimental data showed that the value of $\sigma(s)$ is small ($\approx 10^{-3}$ ps/cm) and it was set equal to zero in further analysis. A value of 82 ± 6 ps was obtained for σ_{trm} . This value is in agreement with the measured trigger time resolution $\sigma_{tr} = 80 \pm 2$ ps but has a larger measurement uncertainty than the directly measured σ_{tr} . Finally the intrinsic PMT resolution was estimated using the formula:

$$\sigma(x) = \sqrt{\sigma_m^2 - \sigma_{tr}^2}. \quad (5)$$

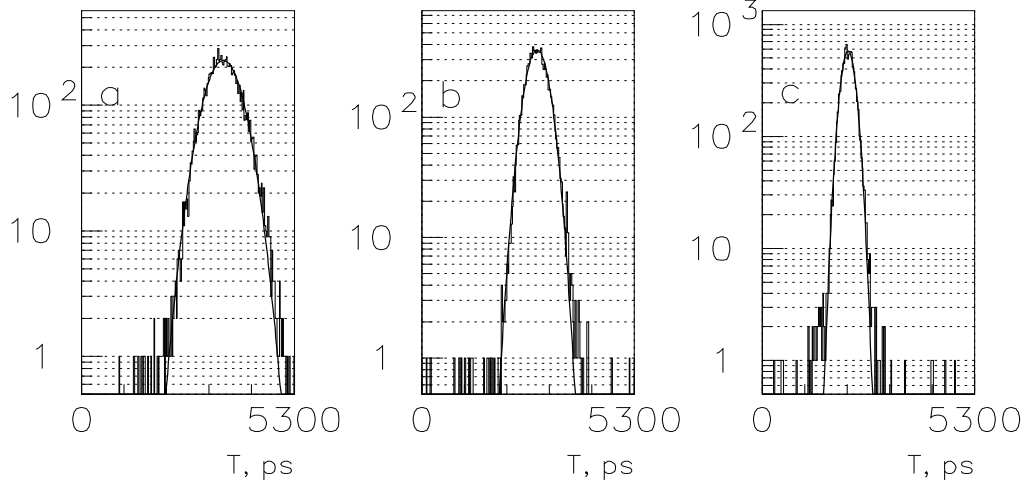


Figure 7. T1 time spectra for (a): $x = -90$; (b): $x = 0$ and (c): $x = 90$ cm. The curves are the result of fits to a Gaussian distribution.

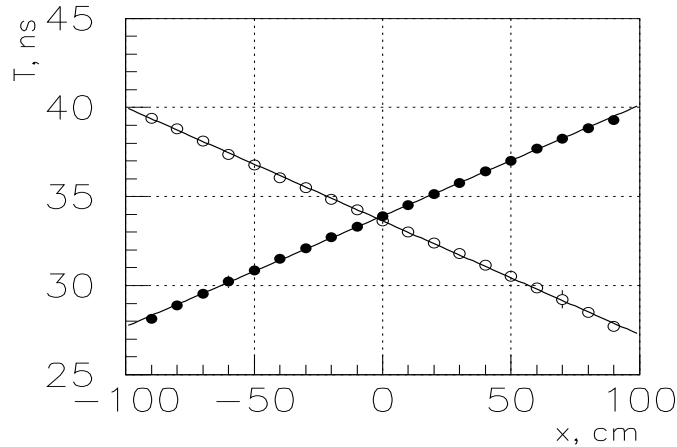


Figure 8. The average time T as a function of x . The fits to a linear dependence yield the velocity of light V_x along the bar.

Fig. 9 shows $\sigma(x)$ for T1. Experimental data are fitted by the following functions:

$$\sigma(x) = \sigma_0 \exp(\pm x/\lambda_t), \quad (6)$$

$$\sigma(x) = \sigma'_o \exp(\pm x/\lambda'_t + \alpha_t x^2/\lambda_t'^2), \quad (7)$$

where ‘+’ and ‘-’ refer to T1 and T2, respectively, $\sigma_o = 209 \pm 1$ ps, $\lambda_t = 113 \pm 2$ cm, $\sigma'_o = 213 \pm 1$ ps, $\lambda'_t = 106 \pm 1$ cm, $\alpha_t = -0.18 \pm 0.02$. Similar values were obtained for T2 as well.

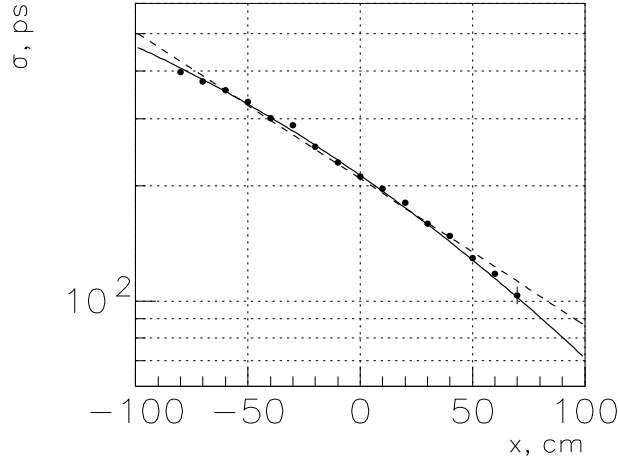


Figure 9. T1 time resolution vs x . The dotted and solid lines fits to equations (6) and (7) respectively.

If the time resolution depends only on photoelectron statistics then $\sigma \sim 1/\sqrt{N_{ph}}$ and $\lambda_t/\lambda_a = 2$, $\alpha_t/\alpha_a = -2$. In our case the first ratio is equal to 1.7 and the second one is -1.1 ± 0.1 . Thus though photoelectron statistics is the main source of the signal time spread some other factors (like photon statistics, etc.) have to be taken into account for precise $\sigma(x)$ estimation for long scintillation counters.

The counter time resolution $\sigma_c(x)$ is shown in Fig. 10. It was calculated using the following relation:

$$\sigma_c(x) = \sqrt{\frac{\sigma_1^2(x) \cdot \sigma_2^2(x)}{\sigma_1^2(x) + \sigma_2^2(x)}}, \quad (8)$$

where subscripts 1 and 2 refer to T1 and T2. The solid line in Fig. 10 uses equation (8) with $\sigma_1(x)$ and $\sigma_2(x)$ given by equation (6). If one neglects the small difference in the time resolutions for T1 and T2 and considers their parameters in equation (6) to be equal to their averages, $\bar{\sigma}_o$ and $\bar{\lambda}_t$, then the following expression is valid:

$$\sigma_c(x) = \frac{\bar{\sigma}_o}{\sqrt{2}} \cosh^{-1/2} \left(\frac{2x}{\bar{\lambda}_t} \right), \quad (9)$$

The dotted line in Fig. 10 shows this dependence with the parameters $\bar{\sigma}_o = 214$ ps and $\bar{\lambda}_t = 107$ cm.

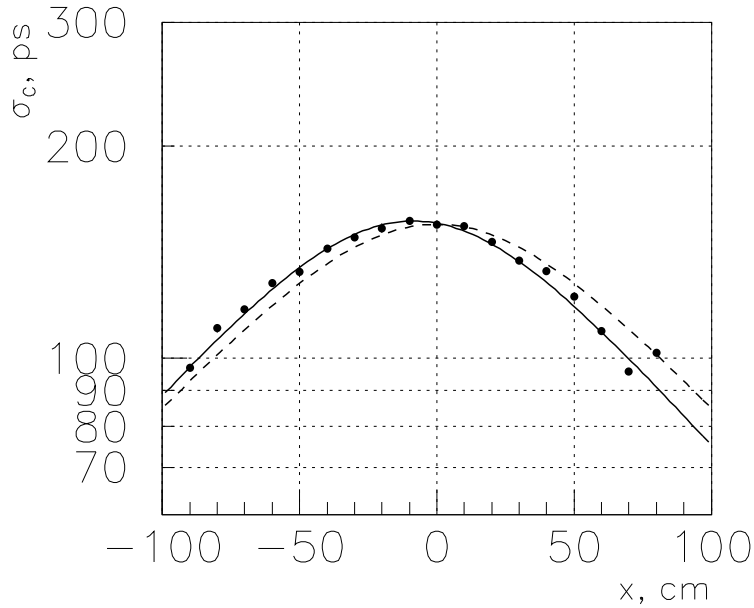


Figure 10. The x -dependence of the counter time resolution $\sigma_c(x)$. The solid and dotted lines represent equations (8) and (9) respectively.

4. Measurements with LED's

To reach the ultimate time resolution available with a CFD it is necessary to carry out fine tuning of its internal delay, threshold and comparison fraction. If the walk-effect correction can be applied in the analysis instead, it may turn out to be more convenient to use simple leading edge discriminators (LED's) and to measure simultaneously signal pulse heights with ADC's. We made measurements that allow us to compare these two options.

CFD parameters were tuned precisely to obtain the best time resolution. LED's based on the fast comparator KP597CA1 [15] were used. LED thresholds were set at 30 mV i.e. 10% of average signal pulse height at $x = 0$. Fig. 11a shows the time spread of T2 signals vs signal pulse heights for $x = 0$ measured with LED. One can see that the measured time T_m depends on the signal pulse height (walk-effect). The following function was used to correct the walk effect:

$$T_c(A) = T_m - b \left(\frac{1}{\sqrt{A}} - \frac{1}{\sqrt{A_o}} \right), \quad (10)$$

where T_c is the corrected time, A is the measured pulse height, A_o is a signal pulse height with zero correction and b is a free parameter depending on x [16]. Fig. 13 demonstrates that there is no correlation between T_c and A . The dependence of $b(x)$ is shown in Fig. 12.

Fig. 13 presents the T2 time resolution vs x measured with CFD and LED. From this figure it follows that the walk-effect correction for LED reduced the time spread by the factor of 1.5 and time resolutions become better than those obtained with CFD except the points at the far end of the scintillator where the contribution of photoelectron statistics to the signal time spread dominates.

It is important that the walk-effect correction makes the time distribution more symmetric and close to the Gaussian (Fig. 14). The asymmetric shape of the time distribution without correction is connected with the Landau tail in the pulse height distribution (see Fig. 3).

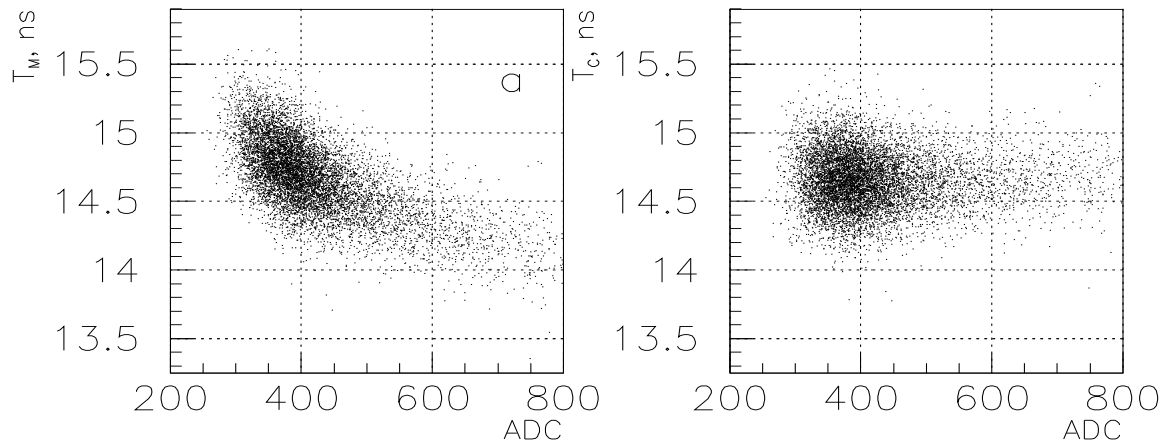


Figure 11. T2 signal time spread vs pulse height (in ADC's counts) for $x = 0$ without (a) and with (b) walk-effect correction for the leading edge discriminator.

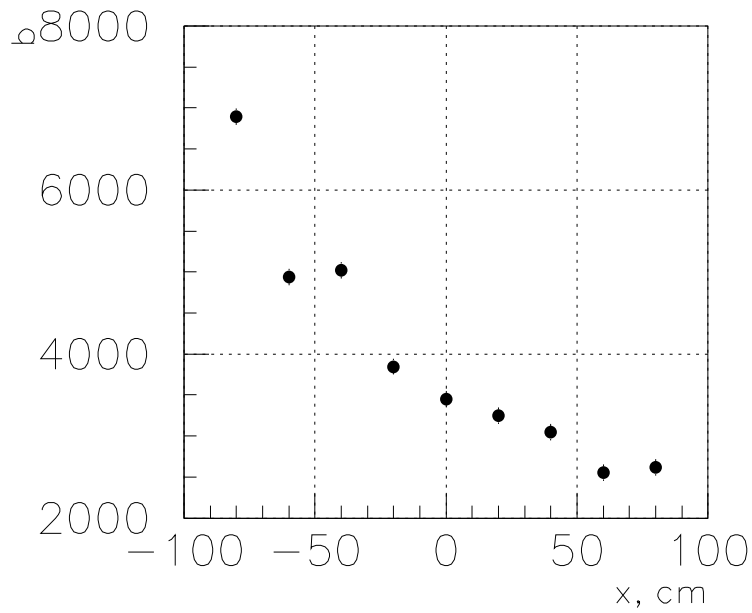


Figure 12. X-dependence of the correction factor b . Signal pulse height A is measured in ADC's counts.

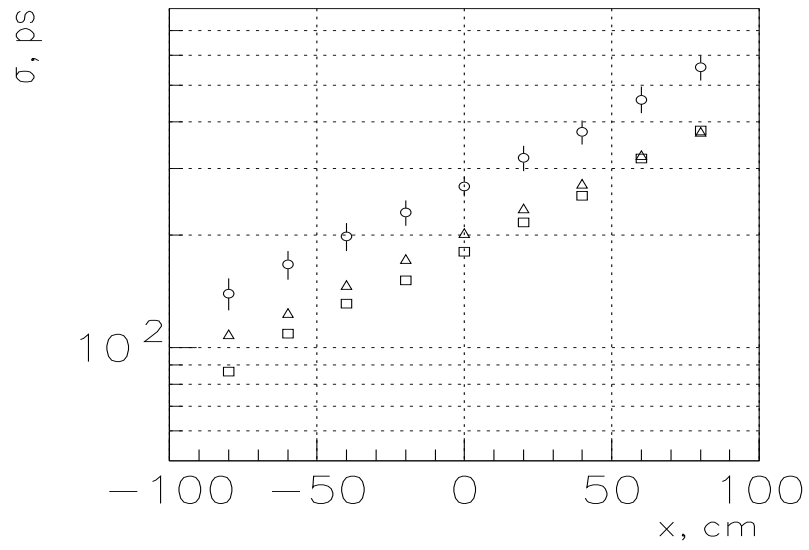


Figure 13. T2 time resolution vs x for LED without (\circ) and with (\square) walk-effect correction and for CFD (\triangle).

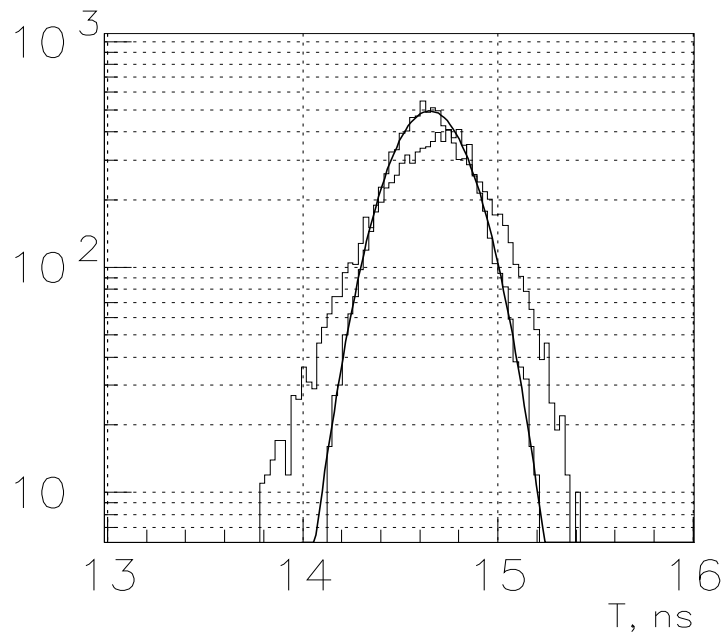


Figure 14. T2 time spectra at $x = 0$ without (histogram) and with walk-correction (histogram fitted using a Gaussian).

5. Conclusions

Detailed studies of the time resolution characterizing a 2 m long scintillation counter were performed in the 5 GeV/c hadron beam of the IHEP accelerator. The scintillator cross-section was $2.5 \times 2.5 \text{ cm}^2$. It was viewed from both ends by FEU-115 PMT's. The number of photoelectrons was measured to be 280 when a relativistic particle passes through the scintillator center. The dependences of the signal pulse height and the time resolution on the distance between the particle trajectory and the PMT are well described by exponential functions with a quadratic term.

The time resolution of the counter is equal to 150 ps at the center and 80 ps near the edges if constant fraction discriminators (CFD) are used. Further improvement of the time resolution in the counter center can be realized by better scintillation light collection achievable by improvement in surface finishing techniques.

The efficacy of using leading edge discriminators with a simultaneous measurement of pulse height was investigated. It was found that this technique resulted in superior time resolution compared to that obtained with constant fraction discriminators.

Acknowledgements

We appreciate financial support from the Russian Ministry for Science and Education (grant 1305.2003.2), from the Russian Foundation for Basic Researches (grant 05-02-16557) and from the US Department of Energy.

References

- [1] Tanimori T. et al. // Nucl. Instr. and Meth. 1983. V. A216. P. 57.
- [2] Sugitate T. et al. // Nucl. Instr. and Meth. 1986. V. A249. P. 354.
- [3] Ferrer A. et al. // Nucl. Instr. and Meth. 1996. V. A317. P. 397.
- [4] Grabmayr P. et al. // Nucl. Instr. and Meth. 1998. V. A402. P. 85.
- [5] www.gluex.org
- [6] www.eljen.com
- [7] www.melz.ct.ru
- [8] L.Aphecetche et al. // Nucl.Instr. and Meth. V. A499 P.521.
- [9] V.Abramov et al. // Nucl.Instr. and Meth. 1998. V. A419. P. 660.
- [10] S.Denisov et al. // Nucl. Instr. and Meth. 2002. V. A478. P. 440.
- [11] www.bicron.com
- [12] www.photonics.com

[13] www.ortec.com

[14] J.E.Moyal. // Nature, Ser. 7, V.46, N^o 374, P. 263. March, 1955.

[15] Agahanian A.A. Integral chips. Energoatomizdat, Moscow, 1983.

[16] S.Denisov et al., // Nucl. Instr. and Meth. 2004. V.494. P. 495.

Received October 3, 2005.

Препринт отпечатан с оригинала-макета, подготовленного авторами.

С.П.Денисов, А.Дзерба, А.К.Клименко и др.

Исследование временных и амплитудных характеристик сцинтилляционного счетчика длиной 2 м с ФЭУ-115М.

Оригинал-макет подготовлен с помощью системы **Л^AT_EX**.

Подписано к печати 06.10.2005. Формат 60 × 84/8.
Офсетная печать. Печ.л. 1,5. Уч.-изд.л. 1,3. Тираж 100. Заказ 96.
Индекс 3649.

ГНЦ РФ Институт физики высоких энергий
142284, Протвино Московской обл.

